Critical properties of the reaction-diffusion model $2A \rightarrow 3A$, $2A \rightarrow 0$

Enrico Carlon,[1,2] Malte Henkel,[1] and Ulrich Schollwöck[3]
[1]*Laboratoire de Physique des Matériaux, CNRS UMR 7556, Université Henri Poincaré Nancy I, Boîte Postale 239, F-54506 Vandœuvre-les-Nancy Cedex, France*
[2]*INFM, Dipartimento di Fisica, Università di Padova, I-35131 Padova, Italy*
[3]*Sektion Physik, Ludwig-Maximilians-Universität München, Theresienstrasse 37/III, D-80333 München, Germany*
(Received 4 January 2000; revised manuscript received 20 September 2000; published 15 February 2001)

The steady-state phase diagram of the one-dimensional reaction-diffusion model $2A \rightarrow 3A$, $2A \rightarrow 0$ is studied through the non-Hermitian density matrix renormalization group. In the absence of single-particle diffusion the model reduces to the pair-contact process, which has a phase transition in the universality class of directed percolation (DP) and an infinite number of absorbing steady states. When single-particle diffusion is added, the number of absorbing steady states is reduced to 2 and the model no longer shows DP critical behavior. The exponents $\theta = \nu_\parallel / \nu_\perp$ and $\beta / \nu_\perp$ are calculated numerically. The value of $\beta / \nu_\perp$ is close to the value of the parity conserving universality class, in spite of the absence of local conservation laws.

DOI: 10.1103/PhysRevE.63.036101 PACS number(s): 05.70.Ln, 05.70.Jk, 64.60.Ht, 02.60.Dc

I. INTRODUCTION

Reaction-diffusion systems have attracted considerable interest in the past few years [1–3]. While at sufficiently high spatial dimensions their critical behavior is correctly described by mean field rate equations, at dimensions below the upper critical dimension, where the effect of fluctuations becomes important, this approach is no longer valid. In this case one has to resort to other methods, such as, for instance, field theory [4], exact calculations via the Bethe ansatz [5], Monte Carlo and cellular automaton simulations (see [2,6] and references therein), or exact diagonalization techniques [7,8]. Recently other types of approach have been proposed such as the density matrix renormalization group [9] and the standard real-space renormalization group [10].

In this paper we study the critical properties of a one-dimensional reaction-diffusion model where the local dynamics is given by the following rules. Consider a single species of particle (A) on a one-dimensional lattice. Each lattice site can be either occupied by a single particle or empty. A single particle may hop to an empty neighboring site (diffusion). Two particles on neighboring sites can either annihilate ($2A \rightarrow 0$) or create a new particle ($2A \rightarrow 3A$) in the case that one of the sites next to the couple is empty. The reaction rates for these processes are defined in Eqs. (1)–(3) below.

Recently, Howard and Täuber [11] discussed a generalized version of the above model where n particles may be created through the reaction $2A \rightarrow (n+2)A$, and with an arbitrary number of particles per site. They employed a field-theoretical approach and found that the theory is not renormalizable. They argued, however, that for all n the model should not be in the directed percolation (DP) universality class. Their conjecture is based on the analysis of the associated master equation and on the massless nature of the corresponding field theory which is at odds with a phase transition of DP type. However, the critical behavior of the system, i.e., its universality class, remained unknown. In the absence of diffusion, with at most one particle per site, the $n=1$ case is the pair-contact process (PCP), where the steady-state phase transition belongs to the DP universality class [12,13].

Here we present a nonperturbative study of the model corresponding to the $n=1$ case of [11]: the PCP model with additional single-particle diffusion, as obtained from density matrix renormalization group (DMRG) calculations. The DMRG algorithm was introduced by White [14] in 1992 to investigate ground state properties of quantum spin chains numerically. Because of its great accuracy, reliability, and the possibility of treating large systems with a limited computational effort, the DMRG has since been applied to an ever increasing set of problems, as reviewed in [15]. In particular, some recent studies were devoted to the application of the DMRG to non-Hermitian problems [9,16–20], which appear frequently in many domains of physics, for example, in low-temperature thermodynamics of spin chains and ladders, for models of the noninteger quantum Hall effect, and in one-dimensional nonequilibrium systems. Reaction-diffusion systems belong to the latter class of models. Some insight should be expected from the application of the DMRG to them [9].

The paper is organized as follows. In Sec. II we define the model and recall some facts about reaction-diffusion systems. In Sec. III we introduce a shift strategy to project out a trivial ground state from the quantum Hamiltonian. This improves the convergence of the DMRG. The method works if an exact expression for the eigenstate is available. In Sec. IV we discuss the calculation of the critical points and exponents for the model and show that the model does not belong to the DP universality class. Section V concludes the paper.

II. MODEL

We consider a one-dimensional lattice of length L with open boundary conditions, as usual in DMRG calculations [15]. The reactions occur with the following rates:

$$\left.\begin{array}{l} AA0 \rightarrow AAA \\ 0AA \rightarrow AAA \end{array}\right\} \quad \text{with rate } \frac{(1-p)(1-d)}{2}, \tag{1}$$

$$AA \to 00 \quad \text{with rate } p(1-d), \tag{2}$$

$$A0 \leftrightarrow 0A \quad \text{with rate } d, \tag{3}$$

and are parametrized by the diffusion constant d and the pair annihilation rate p. This defines the pair-contact process with diffusion (PCPD) model.

For a first qualitative overview, we consider the mean field kinetic equations. To discuss the effects of diffusion we need the kinetic equations in the *pair approximation*; see, e.g., [2]. If $n=n(t)$ is the spatially averaged single-particle density and $c=c(t)$ the spatially averaged pair density, we find

$$\dot{n} = -2(1-d)pc + (1-d)(1-p)(n-c)c/n, \tag{4}$$

$$\dot{c} = -(1-d)pc\frac{2c+n}{n} - 2d\frac{(n-c)(c-n^2)}{n(1-n)} + (1-d)(1-p)(n-c)(1-c)c/[n(1-n)]. \tag{5}$$

In the $d \to 1$ limit, nontrivial steady states occur only for $c(t) \to n(t)^2$ and one recovers the single-site kinetic equation [rescaling time by a factor $(1-d)$]

$$\dot{n} = (1-p)n^2(1-n) - 2pn^2, \tag{6}$$

which expresses the fact that particles may be created only on empty sites. The time dependence of $n(t)$ for large t is

$$n(t) \simeq \begin{cases} n_\infty + \alpha \exp(-t/\tau) & \text{if } p < p_{c,\mathrm{MF}}(1) \\ \sqrt{3/4}\, t^{-1/2} & \text{if } p = p_{c,\mathrm{MF}}(1) \\ 1/(3p-1)t^{-1} & \text{if } p > p_{c,\mathrm{MF}}(1), \end{cases} \tag{7}$$

where $n_\infty = (1-3p)/(1-p)$, $\tau = (1-p)/(1-3p)^2$, $p_{c,\mathrm{MF}}(1) = 1/3$, and α is a constant that depends on the initial conditions. At small p, where the creation process (1) dominates, the system is in the *active* phase with a nonvanishing particle density in the steady state. On the other hand, for p large, the pair annihilation process (2) dominates, the steady-state particle density is zero, and the system is in the *inactive* phase. In the entire inactive phase, and not only at the critical point, the approach toward the steady state is algebraic, rather than exponential as found in most systems.

The same kind of result also holds in the pair approximation with $d \neq 1$. In the steady state, we have $c(\infty) = n(\infty)(1-3p)/(1-p)$. The particle density vanishes along the curve

$$p_{c,\mathrm{MF}}(d) = \begin{cases} \frac{1}{5}(1+3d)/(1-d), & 0 \leqslant d < 1/7 \\ \frac{1}{3}, & 1/7 < d \leqslant 1. \end{cases} \tag{8}$$

Close to criticality, the particle density $n(\infty) \sim p_{c,\mathrm{MF}}(d) - p$, which is the same as found from n_∞ in the $d \to 1$ limit above. However, the pair density

$$c(\infty) \sim \begin{cases} p_{c,\mathrm{MF}}(d) - p, & d < 1/7 \\ [p_{c,\mathrm{MF}}(d) - p]^2, & d > 1/7. \end{cases} \tag{9}$$

There should thus be different universality classes on both sides of the meeting (''tricritical'') point $p_t = 1/3$, $d_t = 1/7$, where $n(\infty) \sim (p_t - p)^2$ and $c(\infty) \sim (p_t - p)^3$ imply modified critical exponents.

The leading long-time behavior along the critical line $p = p_c(d)$ is

$$\begin{cases} n(t) \sim t^{-1/2}, & c(t) \sim t^{-1} & \text{if } d > d_t \\ n(t) \sim t^{-1}, & c(t) \sim t^{-3/2} & \text{if } d = d_t = 1/7 \\ n(t) \sim t^{-1}, & c(t) \sim t^{-1} & \text{if } d < d_t \end{cases} \tag{10}$$

while $n(t) \sim t^{-1}$ and $c(t) \sim t^{-2}$ in the entire inactive phase $p > p_c(d)$. In the active phase, the steady state is approached exponentially.

Although generally believed to be qualitatively correct in sufficiently high dimensions [1–3], kinetic equations cannot provide correct values of the exponents (and often not even the order of the transition) in low dimensions. In one dimension, the exact decay in the inactive phase is $n(t) \sim t^{-1/2}$ [11], where the exponent 1/2 is that of the model $2A \to 0$ [21], which is recovered by taking the limit $p \to 1$ in the rates (1) and (2). However, the pair approximation suggests the presence of distinct universality classes for d large and d small. In addition, the exponent of the time dependence of $n(t)$ for large d equals 1/2 as found exactly for one-dimensional diffusion. This suggests that the upper critical dimension d^* for that transition should be unity (see [22]) but the value of d^* in the PCPD model is not yet known. To what extent are the predictions of the pair approximation, in particular the existence of several distinct universality classes along the transition line, borne out?

An active state with a finite density of particles can be maintained only in the limit $L \to \infty$. On a finite lattice any configuration of particles will decay toward an absorbing configuration in a finite time. There are *two* possible absorbing configurations that the system cannot leave: (i) the empty lattice and (ii) a lattice occupied by one single diffusing particle. If we take $d=0$, we recover the pair-contact process introduced by Jensen [12]. In that case, any particle configuration without nearest-neighbor pairs is absorbing. The number of absorbing states grows exponentially with the chain length L and it is given by the Fibonacci number (see Appendix A). The steady-state properties of the $d=0$ phase transition between the active and inactive phases are described by the directed percolation universality class [12]. However, the dynamical properties of this transition are more subtle and still under active investigation [23,24]. As we shall see, the presence of single-particle diffusion changes the universality class of the transition between the active and inactive phases: for any finite values of d it no longer falls in the DP universality class.

Long ago, Janssen and Grassberger [25] conjectured that a model with a continuous phase transition from a fluctuating active phase into a phase with a single absorbing state and without additional symmetries is in the DP universality class. While it is widely believed that in the presence of local symmetries in the reaction rates there should be a different universality class (normally the PC if the particle number is

locally conserved modulo 2), Park and Park [26] provided a counterexample which shows that even in the presence of local symmetries the steady-state transition can be in the DP universality class. This already indicates that the universality classification might be more subtle than previously thought. The exponents we want to compare with are (see [1,2])

$$\theta = \nu_\parallel/\nu_\perp \simeq 1.5806\ldots, \quad \beta/\nu_\perp \simeq 0.2520\ldots, \quad \text{DP},$$
$$\theta = \nu_\parallel/\nu_\perp \simeq 1.749\ldots, \quad \beta/\nu_\perp \simeq 0.499\ldots, \quad \text{PC}, \tag{11}$$

and are defined as usual from the density $n(p)\sim(p-p_c)^\beta$ and the spatial and temporal correlation lengths $\xi_{\perp,\parallel}\sim(p-p_c)^{-\nu_{\perp,\parallel}}$ (see also Sec. IV).

The stochastic time evolution of the system is determined by the master equation, cast into the form

$$\frac{\partial|P(t)\rangle}{\partial t} = -H|P(t)\rangle, \tag{12}$$

where $|P(t)\rangle$ is a state vector and H is referred to as the ''quantum'' Hamiltonian. For a chain with L sites, H is a stochastic $2^L\times 2^L$ matrix with elements

$$\langle\sigma|H|\tau\rangle = -w(\tau\to\sigma), \quad \langle\sigma|H|\sigma\rangle = \sum_{\tau\neq\sigma} w(\sigma\to\tau),$$

where $|\sigma\rangle$, $|\tau\rangle$ are the state vectors of the particle configurations σ,τ and w are the transition rates.

Since H is non-Hermitian, it has distinct left and right eigenvectors. We will use the notation $|0_r\rangle,|1_r\rangle,\ldots|n_r\rangle$ ($\langle 0_l|,\langle 1_l|,\ldots,\langle n_l|$) for the right (left) eigenvectors of H corresponding to energy levels $E_0,E_1,\ldots,E_n$ ordered according to $\mathrm{Re}\,E_0\leqslant\mathrm{Re}\,E_1\leqslant\cdots\mathrm{Re}\,E_n$, where Re denotes the real part. One has $\langle n_l|m_r\rangle=0$ if $E_n\neq E_m$ and we normalize the states in such a way that $\langle n_l|n_r\rangle=1$.

Steady states are right eigenvectors of H with zero eigenvalue. The two absorbing configurations mentioned above are steady states and given by

$$|0_r\rangle := |000\cdots0\rangle, \tag{13}$$

$$|1_r\rangle := |A00\cdots0\rangle + |0A0\cdots0\rangle + \cdots + |000\cdots A\rangle. \tag{14}$$

Thus, H has two zero eigenvalues $E_0=E_1=0$, while $\Gamma := \mathrm{Re}\,E_2$ is the inverse relaxation time toward the steady state. Furthermore, since H is stochastic,

$$\langle 0_l| := \sum_\sigma \langle\sigma| \tag{15}$$

is a left eigenvector of H with zero eigenvalue.

The calculation of the eigenvalues and eigenvectors of the stochastic Hamiltonian H, from which we will derive the critical properties of the model, is performed by the DMRG algorithm [14,15] adapted to non-Hermitian matrices, as described in detail in Ref. [9]. In the next section we present a further improvement to deal with systems with degenerate ground states.

III. SHIFT OF THE TRIVIAL GROUND STATE

A severe numerical problem is generated by the fact that the physically relevant eigenstate, the first excited state, is only the third state in the spectrum due to the double degeneracy of the ground state. Asymmetric diagonalization algorithms for large sparse matrices are much less robust than their counterparts for symmetric matrices, making a precise determination of eigenvalues not at the extreme ends of the spectrum much more demanding. In particular, the precision of the eigenstates suffers. This in turn leads to a lower-quality truncation of the state space in the DMRG algorithm and subsequently to further deterioration of the results for longer chains. In the present case, the DMRG becomes unstable for rather short chain lengths ($L\approx 20$).

We alleviate this problem successfully by projecting out one of the two ground states, for which both the left and right eigenstate are known, as given in Eqs. (15) and (13). All *nondegenerate* eigenstates of the asymmetric Hamiltonian H obey a biorthogonality condition. This leaves us with two options to eliminate one ground state. (i) Each diagonalization algorithm for large matrices (Arnoldi or Lanczós) generates a sequence of (bi)orthogonal trial vectors, such that the requested eigenstate can be written as a linear combination of those. During the generation, one may enforce orthogonality of all these trial vectors with respect to the ground state. This option does not exist if one uses a black box routine. (ii) One may directly modify the Hamiltonian by shifting the ground state to an arbitrarily high energy, i.e., working with

$$H'(\Delta) := H + \Delta|0_r\rangle\langle 0_l|, \tag{16}$$

where Δ is a positive number larger than the energy gap of H. This new Hamiltonian is not stochastic; however, it has the same spectrum as H apart from one of the ground states which is shifted to an energy level Δ. The gap can now be obtained from the first excited state of $H'(\Delta)$. This procedure can also be implemented for a stochastic Hamiltonian with a single ground state. The gap is then obtained from the ground state energy of $H'(\Delta)$. This option can always be used independently of the diagonalization method employed (see [8] in relation to the power method).

To implement both options, one has to write down the left and right ground states in the transformed block bases generated by the DMRG. Let us denote for a block of length L by $|0_L\rangle$ the state with no particles and by $\langle\tau_L| \equiv \Sigma_{\sigma_L}\langle\sigma_L|$ the sum over all states of a block (i.e., in the complete, unreduced Hilbert space of the block). In the reduced block basis $\{|m_L\rangle\}$ produced by the DMRG we have approximately $|0_L\rangle = \Sigma_{m_L}\langle m_L|0_L\rangle|m_L\rangle$ and $\langle\tau_L| = \Sigma_{m_L}\langle\tau_L|m_L\rangle\langle m_L|$. The right and left ground eigenstates then read

$$|0_r\rangle_{2L+2} = |0_L\rangle\otimes|0\rangle\otimes|0\rangle\otimes|0_L\rangle$$
$$= \sum_{m_L,m_L'} \langle m_L|0_L\rangle\langle m_L'|0_L\rangle(|m_L\rangle \otimes|0\rangle\otimes|0\rangle\otimes|m_L'\rangle), \tag{17}$$

$$\langle 0_l|_{2L+2} = \sum_{s,s'} \langle \tau_L| \otimes \langle s| \otimes \langle s'| \otimes \langle \tau_L|$$

$$= \sum_{m_L, m_L', s, s'} \langle \tau_L | m_L \rangle \langle \tau_L | m_L' \rangle (\langle m_L| \otimes \langle s| \otimes \langle s'| \otimes \langle m_L'|), \tag{18}$$

where s and s' run over single-site states.

At the beginning of the DMRG application, the matrix elements $\langle m_L|0_L\rangle$ and $\langle \tau_L|m_L\rangle$ are trivially constructed for a sufficiently small L such that the Hilbert space has fewer then m states, the number of states kept.

Using $\langle \tau_{L+1}| = \Sigma_s \langle \tau_l| \otimes \langle s|$ and $|0_{L+1}\rangle = |0_L\rangle \otimes |0\rangle$ and inserting one in $\langle \tau_{L+1}| = \Sigma_{m_{L+1}} \langle \tau_{L+1}|m_{L+1}\rangle \langle m_{L+1}|$ and $|0_{L+1}\rangle = \Sigma_{m_{L+1}} \langle m_{L+1}|0_{L+1}\rangle |m_{L+1}\rangle$ one finds as the recursive relation

$$\langle m_{L+1}|0_{L+1}\rangle = \sum_{m_L} \langle m_{L+1}|m_L 0\rangle \langle m_L|0_L\rangle, \tag{19}$$

$$\langle \tau_{L+1}|m_{L+1}\rangle = \sum_{m_L, s} \langle m_L s|m_{L+1}\rangle \langle \tau_L|m_L\rangle. \tag{20}$$

The matrix elements $\langle m_{L+1}|m_L s\rangle$ are from the incomplete basis transformation $|m_L\rangle \otimes |s\rangle \to |m_{L+1}\rangle$.

Numerical implementation of both approaches reveals that the second approach is numerically very stable, while the first one is not, at least not if one carries out an unsophisticated Gram-Schmidt orthogonalization. We suppose that this is due to the fact that global orthogonality of the trial vectors is numerically not exactly conserved by the diagonalization algorithms, while the Gram-Schmidt method assumes this when a new trial vector is added and made orthogonal to the ground state. To find $\Gamma = \mathrm{Re}\, E_2$, we have chosen as density matrix

$$\rho = \frac{1}{4} \widehat{\mathrm{tr}} \{ |0_r\rangle\langle 0_r| + |0_l\rangle\langle 0_l| + |2_r\rangle\langle 2_r| + |2_l\rangle\langle 2_l| \}, \tag{21}$$

where $\widehat{\mathrm{tr}}$ denotes the partial trace on the states of the left or right side of the chain. It is essential to target also the ground state $|0_r\rangle, \langle 0_l|$ projected out to maintain a good description of the ground state via Eqs. (17) and (18) after some DMRG steps. Otherwise, the Hamiltonian still contains a small perturbing contribution from the zero-energy ground state, which might destroy the stability of the procedure.

IV. NUMERICAL RESULTS

A. Analysis of the gap

1. Finite-size scaling method

We are interested in the lowest-energy gap

$$\Gamma = \Gamma(p,d;L) = E_2 \tag{22}$$

whose finite-size scaling behavior contains the desired information about the critical properties of the PCPD model (1)–(3). While in principle the eigenvalues of the (nonsymmetric) matrix H may have a nonzero imaginary part, we always found that E_2 is real.

Generically, we expect the following finite-size behavior of Γ:

$$\Gamma \sim \begin{cases} \exp(-L/\xi_\perp) & \text{if } p < p_c(d) \\ L^{-\theta} & \text{if } p = p_c(d) \\ L^{-2} & \text{if } p > p_c(d) \end{cases} \tag{23}$$

with $\theta = \nu_\parallel / \nu_\perp$ and $\xi_\perp$ the spatial correlation length. At a continuous transition this diverges as $\xi_\perp \sim |p - p_c(d)|^{-\nu_\perp}$, while in the time direction $\xi_\parallel \sim |p - p_c(d)|^{-\nu_\parallel}$.

The first line in Eq. (23) indicates that on a finite lattice the relaxation toward the absorbing configurations is very slow. Indeed, for $L \to \infty$ the relaxation time $\tau = \Gamma^{-1}$ becomes infinite and a state with a finite density of particles becomes a steady state of the system. From the third line in Eq. (23) we see that in the entire inactive phase the scaling behavior of the energy gap is algebraic, with an exponent equal to 2, as for the pair annihilation model $2A \to 0$. Therefore, in addition to the obvious double degeneracy of the ground state, we find that our model is gapless in the large-system limit, $\lim_{L\to\infty} \Gamma(p,d;L) = 0$, for *all* values of p and d (in most systems the gap is finite in the inactive phase).

The different phases and the critical point can be best identified from analysis of the quantity

$$Y_L(p,d) := \frac{\ln[\Gamma(p,d;L+1)/\Gamma(p,d;L-1)]}{\ln[(L+1)/(L-1)]}. \tag{24}$$

While usually the critical point is found by looking for intersections of two curves Y_L and $Y_{L'}$ for two different lattice sizes L, L', it turns out that, because of the scaling (23), *the critical point is found from the maximum of Y_L as a function of p for fixed d and L*. From (23) one then has for the large-L behavior of $Y_L(p,d)$

$$Y_L(p,d) \simeq \begin{cases} -L/\xi_\perp & \text{if } p < p_c(d) \\ -\theta & \text{if } p = p_c(d) \\ -2 & \text{if } p > p_c(d). \end{cases} \tag{25}$$

Therefore, the location of the maximum value of $Y_L(p,d)$ yields a sequence of estimates $p_c(d;L)$ and the critical point can be found from extrapolating these sequences to $L \to \infty$. We point out, however, that the value of Y_L at its maximum *cannot* be used to infer the value of the exponent θ. Only after $p_c(d)$ is determined for the $L \to \infty$ lattice can we use Eq. (25) to find θ. The technicalities of the method are discussed in Appendix B.

2. Inactive phase

Figure 1 shows a plot of $Y_L(p,d)$ as function of the parameter p and for $d = 0.5$ for $L = 9$, 11, 13, 15, and 17 (in the inset we show Y_L for $d = 0.2$). Calculations were performed up to $L = 30$, but for the largest sizes only in the vicinity of the critical point.

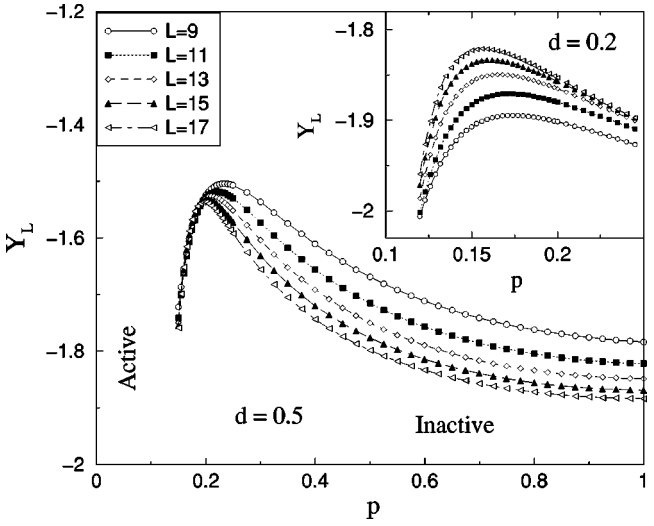

FIG. 1. Plot of $Y_L(p,d)$ as a function of p for various lattice sizes and $d=0.5$. The inset shows the same quantity for $d=0.2$.

In the active phase (small p) the quantity $Y_L(p,d)$ scales linearly with L as predicted in Eq. (25). For larger p the reaction $2A\to 0$ dominates and the system is in the inactive phase, for which we should have asymptotically $Y_L(p,d)\simeq -2$. As the system size L is increased, the curves approach the expected value -2 in the whole inactive phase. Table I shows the values of $-Y_L(p,d)$ calculated for three different diffusion constants and in the inactive phase. We extrapolated the finite-lattice data, using the BST algorithm [27] and found excellent agreement with the expected value of $\theta=2$ [see Eq. (25)]. The convergence is similar to the examples studied in [9], although the raw data can be quite far from their $L\to\infty$ limit value. This check also confirms that the numerical values for the energy gap, as obtained from the DMRG calculation, are very accurate.

3. Active-inactive transition line

Table II collects our results for the critical point $p_c(d)$

TABLE I. Finite-size estimates $-Y_L$ of the dynamical exponent θ and their $L\to\infty$ extrapolation, obtained by the BST method, in the inactive phase.

L	$d=0.1,\ p=0.6$	$d=0.5,\ p=0.6$	$d=0.8,\ p=0.5$
9	1.979223431	1.7110633	1.226133000
11	1.986196898	1.7567773	1.267952170
13	1.990160149	1.7893116	1.306670859
15	1.992629239	1.8139503	1.342357293
17	1.994271913	1.8333674	1.375169517
19	1.995420176	1.8491053	1.405319671
21	1.996254444	1.8621348	1.433037552
23	1.996879687	1.8731052	1.458550029
25	1.997360512	1.8905590	1.482070754
27	1.995400349	1.8976147	1.503795737
29			1.523902146
∞	2.0000(1)	2.000(1)	1.99(2)

TABLE II. Critical parameters $p_c(d)$, θ, and $\beta/\nu_\perp$ along the active-inactive transition line for several values of d.

d	0.10	0.15	0.20	0.35	0.50	0.80
p_c	0.111(2)	0.116(2)	0.121(3)	0.138(1)	0.154(1)	0.205(3)
θ	1.87(3)	1.84(3)	1.83(3)	1.72(3)	1.70(3)	1.60(5)
$\beta/\nu_\perp$	0.50(3)	0.49(3)	0.49(3)	0.47(3)	0.48(3)	0.51(3)

and the exponents θ and $\beta/\nu_\perp$, for several values of d. First, estimates for $p_c(d)$ in the $L\to\infty$ limit were obtained from a linear fit in $1/L$ of the finite-size data $p_c(L)$, i.e., the abscissas of the maxima of $Y_L(p,d)$. For comparison, we recall that $p_c(0)=0.077\,090(5)$ [13].

Next, we estimate the value of the exponent θ from the extrapolation of $\theta_L=-Y_L(p_c(d),d)$ to the thermodynamic limit $L\to\infty$. Figure 2 shows a plot of θ_L as a function of $1/L$ for various values of d. We notice a different finite-size scaling behavior of θ_L for $d\leqslant 0.20$ and for $d=0.50$. In the former case θ_L varies quite strongly with L, starting from a value above 2 and going toward values below 2. For $d\approx 0.5$, θ_L shows little L dependence. The extrapolated values of θ (coming from a cubic fit in $1/L$) are shown in Table II. Error bars are due to the uncertainty in the determination of the critical point location. The final estimates for θ appear to vary with d. It is not yet clear whether this variation is real or the consequence of an unresolved finite-size correction term. However, the results are clearly inconsistent with a transition of DP type, for which $\theta\approx 1.58$.

B. Steady-state particle density

For a finite lattice and for all values of p and d the stationary states, given in Eq. (13) and (14), contain either no or just one particle. Therefore the steady-state particle density vanishes in the large-L limit.

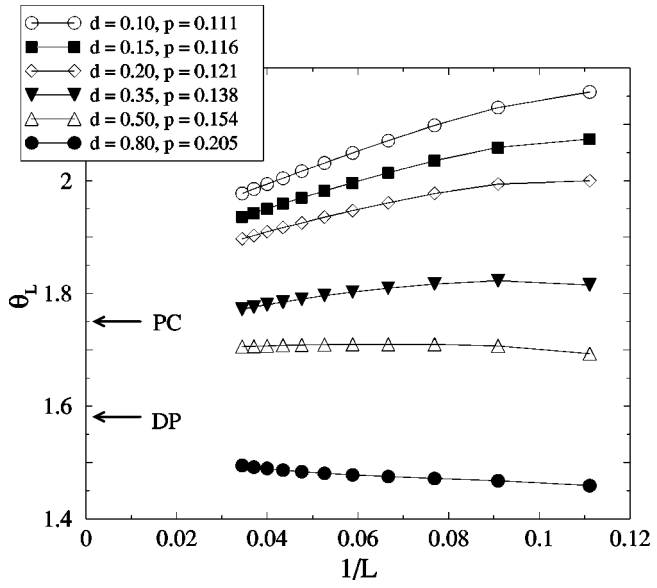

FIG. 2. Plot of θ_L as a function of $1/L$ for various values of d. The two horizontal arrows point to the values of θ expected for the DP ($\theta\approx 1.58$) and PC ($\theta\approx 1.75$) universality classes.

To obtain a steady state with a finite density of particles we added a particle creation process at the two boundary sites [9],

$$0 \to A \quad \text{with rate} \quad p'. \tag{26}$$

We are interested in the (steady-state) density profile, for a chain of length L,

$$n_L(l) = \langle 0_l | \hat{n}(l) | 0_r \rangle, \tag{27}$$

where $l = 1,2,\ldots,L$ labels the position along the chain, $\hat{n}(l)$ is the particle number operator at site l, and $|0_r\rangle$ and $\langle 0_l|$ are the left and right ground states of the nonsymmetric operator H, with the terms coming from Eq. (26) added.

The boundary reaction term removes the ground state degeneracy of H encountered earlier. Therefore, DMRG calculations are easier to perform when $p' \neq 0$. In this case it is not necessary to follow the shift strategy introduced in Sec. III. In fact the DMRG calculations are stable up to chains of length $L \approx 50$–60, i.e., almost double the size of the lengths we could reach in the study of the energy gap.

In general, the time-dependent particle density $n = n(t,p;l,L)$ at site l for a lattice of size L and in the vicinity of the critical point should satisfy the scaling form

$$\begin{aligned} n(t,p;l,L) &= t^{-\beta/\nu_\parallel} F(t/\xi_\parallel, L/\xi_\perp, l/L) \\ &\sim \xi_\perp^{-\beta/\nu_\perp} G(t/\xi_\perp^{\theta}, L/\xi_\perp, l/L), \end{aligned} \tag{28}$$

where for simplicity the dependence on d and p' is suppressed and F and G are scaling functions. The exponents have their usual meaning [2]. In particular, the steady-state density profile, at the critical point, should satisfy

$$n_L(l) := n(\infty, p_c; l, L) = L^{-\beta/\nu_\perp} f(l/L) \tag{29}$$

with some scaling function $f(z)$.

First, we consider the inactive phase. For our model, the average particle density decays algebraically for large times as $n(t) \sim t^{-1/2}$. From Eq. (28), we identify $\beta/\nu_\parallel = 1/2$. Thus $\beta/\nu_\perp = \theta\beta/\nu_\parallel = 1$ since the anisotropy exponent $\theta = \nu_\parallel/\nu_\perp = 2$ in the inactive phase (see Table I).

The scaling (29) is confirmed in Fig. 3, obtained for chains up to $L = 48$, which shows the scaled particle density $Ln_L(l)$ as a function of l/L. The ratio $\beta/\nu_\perp = 1$ for the whole inactive phase has also been confirmed with good accuracy from BST extrapolations.

From now on we focus on the transition between the active and inactive phases. We concentrate on the *central* particle density

$$n(L) := n_L(L/2). \tag{30}$$

For this quantity we expect that for large L, $n(L) \simeq n_0 + O(e^{-L/\xi_\perp}) > 0$ in the active phase where at the critical point

$$n(L) \sim L^{-\beta/\nu_\perp}, \tag{31}$$

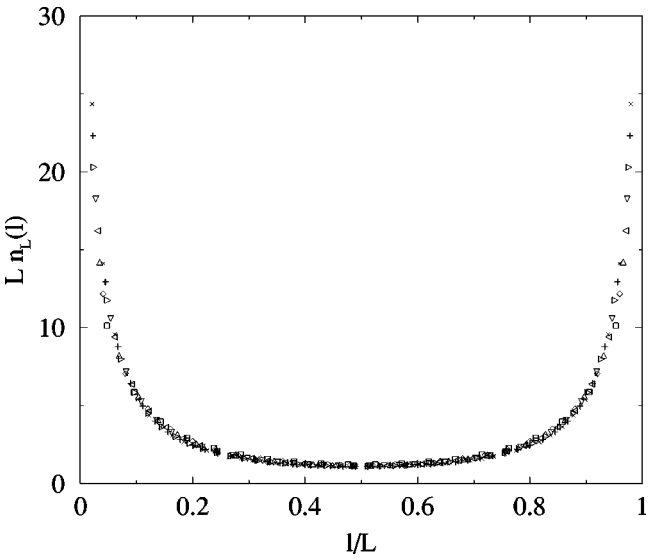

FIG. 3. Scaled particle density $Ln_L(l)$ as function of the scaled variable l/L in the inactive phase for $d = 0.5$, $p = 0.8$, and injection rate $p' = 0.3$. Data for different system sizes ($L = 20,24,28,\ldots,48$) collapse nicely onto a single curve.

while, as shown above, $n(L) \sim L^{-1}$ in the entire inactive phase.

Again, in analogy with Eq. (24) we form the logarithmic derivative

$$\rho(L) = -\frac{\ln[n(L+1)/n(L-1)]}{\ln[(L+1)/(L-1)]}. \tag{32}$$

According to Eq. (31), $\rho(L)$ is expected to converge to the ratio $\beta/\nu_\perp$ for $L \to \infty$ *at* the critical point $p = p_c(d)$ as listed in Table II. A plot of $\rho(L)$ for various values of the diffusion constant is shown in Fig. 4. We notice that at small L and d the effective exponent $\rho(L)$ starts from values close to that for DP, while it clearly deviates from it for increasing L. A cubic fit in $1/L$ yields the extrapolated exponent ratio $\beta/\nu_\perp$ as a function of d (see Table II). This ratio appears to be rather constant with d. As in the case of the calculation of θ, we notice that the exponents are clearly inconsistent with a DP transition. However, the extrapolated values are close to the exponent value expected for a transition in the PC class.

V. DISCUSSION

We collect the results of this study of the pair-contact process with diffusion. In Fig. 5(a) we show the steady-state phase diagram of the PCPD model. For small enough p, there is an active phase with a nonvanishing steady-state particle density and which goes over into an inactive state at some critical point $p_c(d)$. The critical line separating the active from the inactive phase terminates for $d \to 0$ at the DP point $p_c(0) = 0.077\,090(5)$ [13]. For $d \to 1$ the critical line terminates at the MF point $p = 1/3$, as predicted from the mean field equations. This should have been expected, since it is well known that when diffusion dominates over all other reactions the critical behavior becomes of mean field type, even in one dimension [2,3,5].

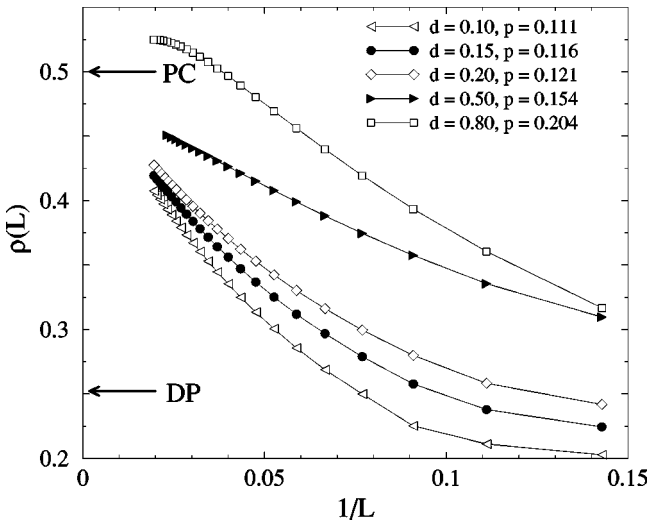

FIG. 4. The effective exponent $\rho(L)$ as a function of $1/L$ for various values of d and for up to $L=51$. The horizontal arrows point to the values expected for DP and for PC universality classes.

In the PCPD model, the entire inactive phase is critical and is expected to be in the universality class of diffusion-annihilation [11]. We have found the exponents $\theta=2$ and $\beta/\nu_\perp=1$, confirming this expectation.

We have investigated the properties of the transition line between the active and inactive phases. Figures 5(b) and 5(c) show the numerical estimates of the exponents θ and $\beta/\nu_\perp$, respectively; see also Table II. For comparison, the values (11) of these exponents for the DP and PC universality classes are shown as horizontal lines. Clearly, our results are incompatible with a transition in the DP class. That means that single-particle diffusion is a relevant perturbation of the pair-contact process. While $\beta/\nu_\perp$ is quite constant and consistent with the PC value within error bars, θ seems to vary continuously with d.

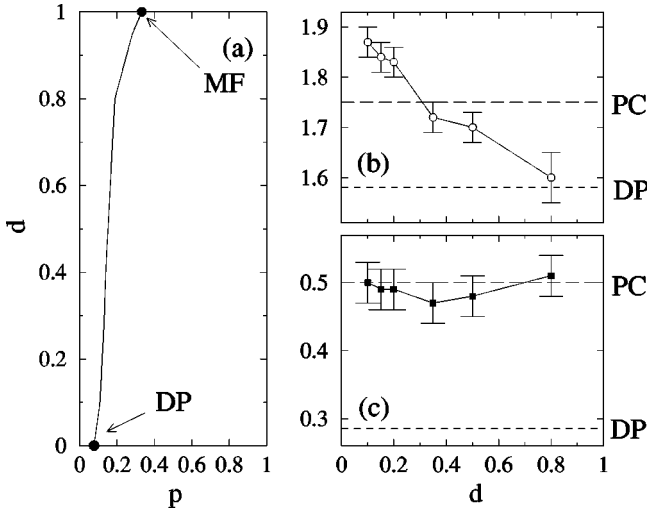

FIG. 5. (a) Steady-state phase diagram of the model $2A\rightarrow 3A$, $2A\rightarrow 0$ as determined by DMRG techniques. The continuous line separates the active from the inactive phase. Extrapolated estimates of the exponent θ are shown in (b) and of the exponent $\beta/\nu_\perp$ in (c) as a function of d.

There is no clear evidence for two distinct universality classes along the critical line, as predicted by pair mean field theory (see Sec. II), but our information on the transition line for d close to unity remains incomplete (see also below). At present, neither of the two possibilities can be ruled out. It is an open question whether the two-dimensional (2D) PCPD model phase diagram will be in qualitative agreement with pair mean field theory.

Turning to the apparent variation of θ with d, note that θ decreases systematically with d, starting from $\theta\approx 2$ in the $d\rightarrow 0$ limit. To explain this, consider the case when d is small and the particle density is low, i.e., the system is close to criticality. Then the particles will diffuse independently until they meet and react. The lower the diffusion rate d, the larger the time interval $t_{\rm diff}$ for which free diffusion can be observed. Associated with this is a length scale $R_{\rm diff}$, viz., $t_{\rm diff}\sim R_{\rm diff}^2$. For times short compared to $t_{\rm diff}$, the system is governed by diffusion only. Therefore, for system sizes $L \ll R_{\rm diff}$, the critical exponents will be effectively those of free diffusion and $\theta\simeq\theta_{\rm diff}=2$. The true value for θ will be seen only if $L\gg R_{\rm diff}$. These two regimes are separated by a crossover region and it appears plausible that the apparent variation of our estimates of θ with d might be the consequence of such a crossover. However, this crossover phenomenon does not show up in the calculation of $\beta/\nu_\perp$. That is to be expected since by injecting particles at the boundaries we induce a *finite* density of particles at the critical point also; $t_{\rm diff}$ will no longer increase beyond any bounds as $d\rightarrow 0$, and the above heuristic argument no longer applies.

While the exponent $\beta/\nu_\perp$ is not far from that of the PC class it is difficult to extract reliable information from θ. We have no reason to believe that exponents should be continuously varying as functions of the diffusion constant. A closer inspection of the finite-size behavior (see Fig. 2) reveals that the $L\rightarrow\infty$ asymptotic value of θ is approached from above for $d\leqslant 0.35$, while it is approached from below for $d\geqslant 0.5$. As finite-size effects are seen to be weak in the interval $0.35\leqslant d\leqslant 0.5$, we presume that the most reliable estimates for θ might be those obtained in this range of diffusion constants. Therefore most likely $\theta\approx 1.7$, which is not far from the PC value either. We also recall that the relaxation in the inactive phase is algebraic: All known models [26,28–31] in the PC class are characterized by an algebraic relaxation in the inactive phase with exponents $\theta=2$ and $\beta/\nu_\perp=1$, as for the PCPD model. Therefore, it might be tempting to speculate that the active-inactive transition of the PCPD model is in the PC universality class.

On the other hand all known models in the PC universality class are characterized by some conservation laws either on the parity of the number of particles or by an exact symmetry between the absorbing states [3]. Such local consevation laws are, however, lacking for the PCPD model, which suggests that the PCPD model should not be in the PC class. It should also be stressed that the unambiguous identification of a steady-state universality class requires the determination of *four* independent exponents (see [2,3]), while our techniques provided values for only two.

In summary, we have used the DMRG method to find the steady-state phase diagram of the PCPD model. Single-

particle diffusion is a relevant perturbation for the system since the model does not show a DP behavior as in the limit of vanishing diffusion constant.

Some exponent values along the active-inactive transition line are surprisingly close to those of the PC universality class. However, it is conceivable that the near coincidence of the exponents with those of the PC class might be accidental. In that case the transition(s) would belong to a universality class distinct from both DP and PC. It is not yet clear whether in the 1D PCPD model there are two distinct transitions, as suggested by pair mean field theory, or merely a single one. All in all, complementary studies would be needed to fully understand the remarkably subtle behavior of this so simple-looking model.

After this work was done Hinrichsen [32] performed a Monte Carlo study of the PCPD model for $d=0.1$. The time-dependent density $n(t)\sim t^{-\delta}$ is characterized by the exponent $\delta=\beta/(\nu_\perp\theta)$. He finds $\delta=0.25(2)$ and $\theta=1.83(5)$. This agrees with our Table II. After this work was accepted, we received a paper by Ódor [33] which studies the PCPD model through Monte Carlo simulations and the coherent anomaly method. In particular, for $0.05\leqslant d\leqslant 0.2$, Ódor finds $\delta\approx 0.27$, and for $d=0.5$ and $d=0.9$, $\delta\approx 0.2$. The first result compares well with our results from Table II, which give $\delta\approx 0.27$, and agrees with the result of Hinrichsen [32]. However, Odor also finds $\beta\approx 0.58$ for $0.05\leqslant d\leqslant 0.2$, consistent with the upper bound $\beta<0.67$ reported in [32]. That is far away from the PC value $\beta_{\rm PC}\simeq 0.93$ [2,31].

ACKNOWLEDGMENTS

It is a pleasure to thank P. Grassberger, H. Hinrichsen, M. Howard, J. F. F. Mendes, G. Ódor, U. Täuber, and F. van Wijland for many stimulating discussions and J. F. F. Mendes for participation in the earliest stages of this work. We thank H. Hinrichsen in particular for a useful discussion about Eq. (25). M. H. thanks the Department of Theoretical Physics of the University of Oxford, where early stages of this work were performed, for warm hospitality and J. L. Cardy and Z. Racz for discussions. We thank the Centre Charles Hermite in Nancy for providing substantial computational time. E.C. acknowledges partial financial support by the Ministère des Affaires Etrangères Grant No. 224679A. M.H. and U.S. were supported in part by the Procope program.

APPENDIX A: NUMBER OF ABSORBING CONFIGURATIONS IN THE PCP

For $d=0$, the model reduces to the pair contact process [12]. In this case, all configurations of the type $|\ldots 0A0\ldots 0A0\ldots\rangle$ without nearest-neighbor particles are absorbing and stationary states. We find the number $N(L)$ of absorbing states in the PCP for a chain of length L with free (periodic) boundary conditions.

For *free* boundary conditions, one has the recursion

$$N(L)=N(L-1)+N(L-2). \tag{A1}$$

To see this, concentrate on the leftmost site. If it is occupied, its neighbor must be empty for the state to be absorbing and there remains an open chain of $L-2$ sites to be considered. If it is empty, one considers the open chain of the remaining $L-1$ sites. The initial conditions for the problem are $N(1)=2$ and $N(2)=3$. Therefore $N(L)=F_{L+1}$ is the $(L+1)$th Fibonacci number.

This can also be seen from the generating function

$$\tilde{N}(s)=\sum_{k=0}^{+\infty} N(k)s^k \tag{A2}$$

which satisfies, because of Eq. (A1),

$$\tilde{N}(s)=\frac{N(0)(1-s)+N(1)s}{1-s-s^2}=\frac{1+s}{1-s-s^2}. \tag{A3}$$

For the inverse transformation one can use

$$N(L)=\frac{1}{2\pi \mathrm{i}}\oint ds\tilde{N}(s)s^{-L-1}, \tag{A4}$$

where the integral is taken in a closed circle centered at the origin of the complex s plane and with radius smaller than the radius of convergence of the series (A2), so as to exclude contributions of other poles than that in $s=0$. The transformation $z=1/s$ yields

$$N(L)=\frac{1}{2\pi i}\oint dz\frac{1+z}{z^2-z-1}z^L=\frac{z_+^{L+2}-z_-^{L+2}}{z_+-z_-}, \tag{A5}$$

where $z_\pm=(1\pm\sqrt{5})/2$; z_+ is the golden mean.

For *periodic* boundary conditions, the number $N_{\rm per}(L)$ of absorbing states for a chain of L sites is

$$N_{\rm per}(L)=N(L-1)+N(L-3)=z_+^L+z_-^L. \tag{A6}$$

For large L the asymptotic behavior is $N(L)\sim N_{\rm per}(L)\sim z_+^L$.

Another example of a kinetic model with exponentially many absorbing states is an adsorption-desorption model of k-mers ($k\geqslant 3$) on a 1D lattice where the number of absorbing states is described by generalized Fibonacci numbers [34].

APPENDIX B: FINITE-SIZE SCALING IN SYSTEMS WITH A CRITICAL PHASE

We discuss the finite-size scaling of the lowest gap $\Gamma=\Gamma_L(p)$ and how to localize the critical point. For simplicity, we suppress the dependence on d and write the scaling form

$$\Gamma_L(p)=L^{-\theta}f[(p-p_c)L^{1/\nu_\perp}], \tag{B1}$$

where f is assumed to be continuously differentiable. For the gap, one expects the behavior

$$\Gamma_L(p) \sim \begin{cases} e^{-\sigma L} & \text{if } p < p_c \\ L^{-2} & \text{if } p > p_c, \text{ case } C \\ \Gamma_\infty & \text{if } p > p_c, \text{ case } N, \end{cases} \tag{B2}$$

where σ, Γ_∞ are constants independent of L. Here, case N refers to the ''normal'' case of noncritical phases on both sides of the transition at $p = p_c$ and case C alludes to the case of a critical phase on one side, and we have already set the exponent equal to 2 in view of Eq. (23), valid for our model. This implies for the scaling function $f(z)$

$$f(z) \sim \begin{cases} \exp(-A|z|^{\nu_\perp}), & z \to -\infty \\ z^{(\theta-2)\nu_\perp}, & z \to +\infty, \text{ case } C \\ z^{\theta\nu_\perp}, & z \to +\infty, \text{ case } N, \end{cases} \tag{B3}$$

where A is a positive constant. Since $f(z)$ is positive, it follows that in the case C with $\theta < 2$ $f(z)$ must have a maximum at some finite value $z_{\max}$. For the case N, however, $f(z)$ should increase monotonically with z.

The estimator Y_L as defined in Eq. (24) then becomes

$$Y_L = -\theta + \frac{\ln[f(z_+)/f(z_-)]}{\ln[(L+1)/(L-1)]}, \tag{B4}$$

where $z_\pm = (p - p_c)(L \pm 1)^{1/\nu_\perp}$. Furthermore, writing $g(z) = \ln f(z)$, a straightforward calculation gives

$$\lim \frac{dY_L}{dp} = \frac{L^{1/\nu_\perp}}{\nu_\perp}[g'(z) - z g''(z)] \simeq \begin{cases} L^{1/\nu_\perp} A(2-\nu_\perp)(-z)^{\nu_\perp - 1}, & z \to -\infty \\ L^{1/\nu_\perp}(\theta - 2) z^{-1}, & z \to \infty \end{cases} \tag{B5}$$

in the finite-size scaling limit $p \to p_c$ and $L \to \infty$ simultaneously such that $z = (p - p_c)L^{1/\nu_\perp}$ is kept fixed. For the case C with $\theta < 2$ and $\nu_\perp < 2$, there is some finite z^* such that $dY_L/dp|_{z=z^*} = 0$. Then

$$Y_L(z^*) = -\theta + \frac{1}{\nu_\perp} z^* g'(z^*). \tag{B6}$$

If we choose $z = z^*$, we have a sequence of values of p_L converging toward p_c according to $p_L \simeq p_c + z^* L^{-1/\nu_\perp}$. On the other hand, p_L *can be found by determining the maximum of* Y_L *as a function of* p, since $\lim dY_L/dp|_{z^*} = 0$. This is the desired result. However, because of Eq. (B6) $Y_L(z^*)$ does *not* readily yield an estimate for the exponent θ, since there is no guarantee that $g'(z^*)$ should vanish (or in other words that $z^* = z_{\max}$). The generalization to other observables with scaling analogous to (B2) is immediate. For the case N, however, this technique does not apply, since in general $f'(z) > 0$ for all values of z.

Finally, we recall that the leading finite-size correction terms determine whether or not the curves $Y_L(p)$ and $Y_{L'}(p)$ will intersect. Consider the extended scaling form $\Gamma_L(p) = L^{-\theta} f(z)[1 + L^{-\omega} A(z)]$, where $\omega > 0$ is the leading correction exponent. If $\omega < 2$, we find

$$Y_L = -\theta + \frac{z g'(z)}{\nu_\perp} + L^{-\omega} A(z) \left(-\omega + \frac{1}{\nu_\perp} \frac{z A'(z)}{A(z)} \right) \tag{B7}$$

up to terms of order $O(L^{-2}, L^{-1-\omega})$. Now, the curves Y_L and $Y_{L'}$ intersect if there is some z_{int} such that the scaling function of the leading correction term in Eq. (B7) vanishes. But that term depends *only* on the correction amplitude $A(z)$ and is independent of $f(z)$.

[1] *Nonequilibrium Statistical Mechanics in One Dimension*, edited by V. Privman (Cambridge University Press, Cambridge, 1996).

[2] J. Marro and R. Dickman, *Nonequilibrium Phase Transitions in Lattice Models* (Cambridge University Press, Cambridge, 1999).

[3] H. Hinrichsen, Adv. Phys. **49**, 1 (2000).

[4] J. Cardy and U. C. Täuber, Phys. Rev. Lett. **77**, 4780 (1996); J. Stat. Phys. **90**, 1 (1998); D. C. Mattis and M. L. Glasser, Rev. Mod. Phys. **70**, 979 (1998).

[5] D. Kandel, E. Domany, and B. Nienhuis, J. Phys. A **23**, L755 (1990); F. C. Alcaraz, M. Droz, M. Henkel, and V. Rittenberg, Ann. Phys. (N.Y.) **230**, 250 (1994); I. Peschel, U. Schultze, and V. Rittenberg, Nucl. Phys. B **430**, 633 (1995); P.-A. Bares and M. Mobilia, Phys. Rev. Lett. **83**, 5214 (1999); **85**, 893 (2000); G. M. Schütz, in *Phase Transitions and Critical Phenomena*, edited by C. Domb and J. L. Lebowitz, Vol. 19 (Academic Press, New York, 2000).

[6] B. Chopard and M. Droz, *Cellular Automata Modelling of Physical Systems* (Cambridge University Press, Cambridge, 1998).

[7] M. Henkel and H. Herrmann, J. Phys. A **23**, 3719 (1990); J. R. G. de Mendonça, Phys. Rev. E **60**, 1329 (1999).

[8] J. R. G. de Mendoną, J. Phys. A **32**, L467 (1999).

[9] E. Carlon, M. Henkel, and U. Schollwöck, Eur. Phys. J. B **12**, 99 (1999).

[10] J. Hooyberghs and C. Vanderzande, J. Phys. A **33**, 907 (2000).

[11] M. J. Howard and U. C. Täuber, J. Phys. A **30**, 7721 (1997).

[12] I. Jensen, Phys. Rev. Lett. **70**, 1465 (1993).

[13] R. Dickman and J. Kamphorst Leal da Silva, Phys. Rev. E **58**, 4266 (1998).

[14] S. R. White, Phys. Rev. Lett. **69**, 2863 (1992); Phys. Rev. B **48**, 10 345 (1993).

[15] *Density Matrix Renormalization: A New Numerical Method in*

Physics, edited by I. Peschel, X. Wang, M. Kaulke, and K. Hallberg (Springer, Heidelberg, 1999).

[16] R. J. Bursill, T. Xiang, and G. A. Gehring, J. Phys.: Condens. Matter **8**, L583 (1996); X. Wang and T. Xiang, Phys. Rev. B **56**, 5061 (1997); N. Shibata, J. Phys. Soc. Jpn. **66**, 2221 (1997); K. Maisinger and U. Schollwöck, Phys. Rev. Lett. **81**, 445 (1998).

[17] Y. Hieida, J. Phys. Soc. Jpn. **67**, 369 (1998).

[18] M. Kaulke and I. Peschel, Eur. Phys. J. B **5**, 727 (1998).

[19] Ö. Legeza, M. Kaulke, and I. Peschel, Ann. Phys. (Leipzig) **8**, 153 (1999).

[20] J. Kondev and J. B. Marston, Nucl. Phys. B **497**, 639 (1997); J. B. Marston and Shan-Wen Tsai, Phys. Rev. Lett. **82**, 4906 (1999); T. Senthil, J. B. Marston, and M. P. A. Fisher, Phys. Rev. B **60**, 4245 (1999); Shan-Wen Tsai and J. B. Marston, Ann. Phys. (Leipzig) **8**, 261 (1999).

[21] L. Peliti, J. Phys. A **19**, L365 (1986).

[22] B. P. Lee, J. Phys. A **27**, 2633 (1994).

[23] I. Jensen and R. Dickman, Phys. Rev. E **48**, 1710 (1993); J. F. F. Mendes, R. Dickman, M. Henkel, and M. C. Marques, J. Phys. A **27**, 3019 (1994); M. A. Muñoz, G. Grinstein, R. Dickman, and R. Livi, Phys. Rev. Lett. **76**, 451 (1996); P. Grassberger, H. Chaté, and G. Rousseau, Phys. Rev. E **55**, 2488 (1997).

[24] R. Dickman, e-print cond-mat/9909347.

[25] H. K. Janssen, Z. Phys. B: Condens. Matter **42**, 151 (1981); P. Grassberger, *ibid.* **47**, 365 (1982).

[26] H. Park and H. Park, Physica A **221**, 97 (1995).

[27] R. Burlisch and J. Stoer, Numer. Math. **6**, 413 (1964); M. Henkel and G. Schütz, J. Phys. A **21**, 2617 (1988).

[28] P. Grassberger, F. Krause, and T. von der Twer, J. Phys. A **17**, L105 (1984); P. Grassberger, *ibid.* **22**, L1103 (1989).

[29] N. Menyhárd, J. Phys. A **27**, 6139 (1994).

[30] N. Inui and A. Yu. Tretyakov, Phys. Rev. Lett. **80**, 5148 (1998); M. C. Marques and J. F. F. Mendes, Eur. Phys. J. B **12**, 123 (1999).

[31] H. Hinrichsen, Phys. Rev. E **55**, 219 (1997).

[32] H. Hinrichsen, following article, Phys. Rev. E **63**, 036102 (2001).

[33] G. Ódor, Phys. Rev. E (to be published).

[34] M. Barma, M. D. Grynberg, and R. B. Stinchcombe, Phys. Rev. Lett. **70**, 1033 (1993).